Reconfigurable Radar Waveform Generation Based on an Optically Injected Semiconductor Laser

Pei Zhou, *Student Member, IEEE*, Fangzheng Zhang, *Member, IEEE*, Qingshui Guo, Simin Li, and Shilong Pan, *Senior Member, IEEE*

***Abstract*—We propose and experimentally demonstrate an approach to generating reconfigurable radar waveforms based on an optically injected semiconductor laser. In the proposed system, the semiconductor laser is operated at period-one oscillation state, in which an optical output signal containing a microwave modulation on the intensity is generated. After photo detection, a frequency-tunable microwave signal is obtained with its instantaneous frequency determined by the optical injection strength and/or the detuning frequency between the master and slave lasers. Since the dynamical behavior of a semiconductor laser evolves at a subnanosecond time scale, by properly designing a control signal to manipulate the optical injection strength, reconfigurable microwave waveforms with desired parameters can be generated for radar and other applications. In particular, the generation of continuous-wave or pulsed, linearly chirped, and frequency-hopping microwave waveforms with reconfigurable parameters are experimentally demonstrated. In addition, a high-resolution distance measurement experiment is performed to verify the feasibility of applying the proposed microwave waveform generator to radar applications.**

***Index Terms*—Microwave generation, microwave photonics, optical injection, radar, semiconductor laser dynamics.**

I. Introduction

MICROWAVE waveform generator is one of key components in microwave and millimeter-wave systems such as spread-spectrum wireless communications [1], modern instrumentation, radars [2], [3] and electronic warfare systems. For radar applications, different microwave waveforms are required for different purposes, which typically include single-frequency pulse trains, linearly chirped continuous wave, linearly chirped pulse trains, and frequency hopping sequences [2]. While these microwave waveforms can be separately generated, having a system that can easily generate diverse microwave waveforms and flexibly switch among one another is highly desired, especially in a multifunction radar system [4]. On the other hand, since the microwave waveform generator in conventional radar systems usually consists of fixed microwave components, which operates efficiently only in a particular frequency band with specific bandwidth. For instance, although a direct digital synthesizer (DDS) [5] can generate reconfigurable microwave waveforms in the electrical domain, it always has a limited central frequency and a bandwidth of a few gigahertz.

To deal with the problems associated with the electronic methods, numerous photonic approaches have been proposed to generate microwave waveforms with high frequency and large bandwidth [6]–[11]. One method is based on direct space-to-time (DST) pulse shaping [6], [7], which is implemented by a broadband laser source, two diffraction gratings and a spatial light modulator (SLM). The problems associated with this system are its complicated configuration, large size, and high coupling loss because it is implemented using expensive and complex free-space optical devices. Another optical scheme for microwave waveform generation is realized based on an optical spectral shaper and a dispersive element for frequency-to-time mapping (FTM) [8], [9]. In such systems, the optical spectrum of a pulsed optical source is first manipulated by a spectral shaper, e.g., a fiber Bragg grating (FBG), before FTM in the dispersive element. But the spectral response of the optical spectral shaper is usually fixed, resulting in the generation of microwave waveforms with either fixed parameters or very limited tunability. External phase modulation followed by optical heterodyning is a promising approach for photonic generation of diverse microwave waveforms [10], [11]. The basic idea for this kind of method is to introduce different phase modulations to two coherent optical wavelengths followed by optical heterodyning in a photodetector (PD). The two lights can be spatially separated or orthogonally polarized. Drawback of this method is that the generated waveform shape and bandwidth are determined by the electrical driving signal. Thus, a high-speed microwave arbitrary waveform generator (AWG) is required, which would increase the system complexity and cost.

Recently, a new photonic approach to generating microwave signals was proposed based on period-one (P1) oscillation in semiconductor lasers [12]–[19]. Under continuous-wave (CW) optical injection, P1 dynamics can be excited through undamping the relaxation resonance of semiconductor lasers. The output intensity of semiconductor lasers exhibits self-sustained

Manuscript received February 1, 2017; revised April 6, 2017 and April 25, 2017; accepted April 25, 2017. This work was supported in part by the National Natural Science Foundation of China under Grants 61401201, 61422108, and 61527820, in part by the NSFC program of Jiangsu Province under Grant BK20140822, in part by the Aviation Science Foundation of China under Grant 2015ZC52024, in part by the Open Fund of Science and Technology on Monolithic Integrated Circuits and Modules Laboratory under Grant 20150C1404, and in part by the Fundamental Research Funds for the Central Universities. *(Corresponding authors: Fangzheng Zhang and Shilong Pan.)*

The authors are with the Key Laboratory of Radar Imaging and Microwave Photonics (Ministry of Education), Nanjing University of Aeronautics and Astronautics, Nanjing 210016, China (e-mail: zhou_pei@nuaa.edu.cn; zhangfangzheng@nuaa.edu.cn; zzckgqs@126.com; lisimin@nuaa.edu.cn; pans@ieee.org).

Color versions of one or more of the figures in this paper are available online at http://ieeexplore.ieee.org.

Digital Object Identifier 10.1109/JSTQE.2017.2699659

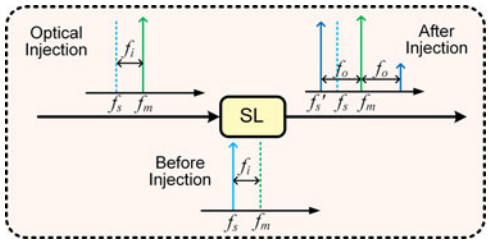

Fig. 1. Schematic diagram of an optically injected semiconductor laser and its spectral characteristic in period-one state. SL: slave laser.

microwave oscillation. The optical spectrum consists of highly intensity-asymmetric sidebands that are equally separated by the P1 oscillation frequency. By properly varying the optical injection strength, the detuning frequency, or both, the microwave frequency generated through P1 oscillation can be continuously tuned from a few to tens or even hundreds of gigahertz. Besides, the unique characteristics of P1 dynamics have also been studied for photonic microwave amplification, single-sideband (SSB) modulation, and optical frequency conversion [20]–[22].

While many studies have been done to achieve single-frequency microwave signal generation, there is little investigation on wideband microwave waveform generation through period-one oscillation. In this work, we propose and experimentally demonstrate a scheme to generating reconfigurable radar waveforms based on an optically injected semiconductor laser. In the proposed system, the optically injected semiconductor laser is operated at period-one oscillation state where an optical output that contains a microwave modulation on the optical carrier is generated. After optical-to-electrical conversion, a microwave signal can be generated with a broadly tunable frequency (i.e., P1 frequency) by varying the optical injection strength and/or the detuning frequency between the master and slave lasers. Because the dynamical behavior of a semiconductor laser evolves at a sub-nanosecond time scale, it provides a convenient way to control the instantaneous frequency of the generated microwave signal by manipulating the optical injection strength. In the proposed configuration, an intensity modulator is inserted to modulate the optical injection strength. By properly designing the control signal to adjusting the optical injection strength, reconfigurable microwave waveforms can be generated for radar and other applications. In particular, the photonic generation of CW/pulsed, linearly chirped or frequency-hopping microwave waveforms are experimentally demonstrated. The parameters of the generated microwave waveforms, including central frequency, bandwidth, temporal duration, frequency band, and duty cycle, are also controllable. To further investigate the performance of the proposed radar waveform generator based on the optically injected semiconductor laser, its application in a radar system is experimentally studied, showing a ranging accuracy of less than 1 cm and a resolution of $\sim$2.46 cm.

II. Principle and Experimental Setup

Fig. 1 shows the schematic diagram of an optically injected semiconductor laser and its spectral characteristic in period-one state. The free-running frequency of the semiconductor laser (slave laser) is f_{s}. A CW light with a frequency of f_{m} (master laser) is injected into the slave laser. P1 dynamics can be invoked through undamping the relaxation resonance of the semiconductor laser. The injection light pulls the intracavity field oscillation of the slave laser toward f_{m} by locking the optical phase of the laser, leading to a frequency component at f_{m} at the laser output. On the other hand, the necessary gain for the slave laser is modified by the optical injection. The refractive index inside the cavity changes through the antiguidance effect, resulting in the redshift of the cavity resonance from f_{s} toward f_{s}' [15]. Therefore, such injection-shifted cavity resonance competes dynamically with the injection-imposed laser oscillation, which radically modifies the dynamics of the injected laser. Under proper injection conditions, this would lead to the emergence of asymmetric double-sideband spectrum that is equally separated by the P1 oscillation frequency f_{o} ($f_{\mathrm{o}} = f_{\mathrm{m}} - f_{\mathrm{s}}'$) through Hopf bifurcation. As indicated in Fig. 1, such spectral characteristic is a signature of P1 dynamics in optically injected semiconductor lasers [12]–[23]. After optical-to-electrical conversion, a microwave signal having a frequency of f_{o} can be generated. Since the cavity resonance shift depends on the gain reduction which is determined by the injection strength and the detuning frequency between the master and slave lasers, the beating microwave frequency is dependent on the injection condition. Here, the injection strength is characterized by ξ, which is defined as the square root of the power ratio between the injected light and the free-running slave laser, i.e., the injection strength ξ is proportional to the optical amplitude of the light injected into the slave laser. For a fixed master-slave detuning frequency f_{i} ($f_{\mathrm{i}} = f_{\mathrm{m}} - f_{\mathrm{s}}$), the microwave frequency f_{o} would increase approximately linearly with the injection strength ξ over a large range, which has been verified both numerically and experimentally in previous reports [12], [17]. Thanks to the fast dynamical rate parameters, the dynamical behavior of a typical semiconductor laser evolves at a sub-nanosecond time scale [13]. Therefore, it provides a convenient way to dynamically control the instantaneous frequency of the generated microwave signal [13], [18], [19]. If an electrical control signal is applied to an intensity modulator (IM) to manipulate the amplitude of the injection light before it is sent to the slave laser, the resultant microwave frequency f_{o} will temporally varies correspondingly. By properly designing the control signal, reconfigurable microwave waveforms can be generated for radar and other applications. For example, by setting the control signal to have a near-sawtooth profile, the injected light can have a linearly increased optical amplitude, and the generated microwave signal would also have a linearly increased frequency, i.e., a linearly chirped microwave waveform is generated. Furthermore, the parameters of the generated microwave waveforms are also reconfigurable, including frequency band, central frequency, bandwidth, temporal duration and duty cycle. For instance, the bandwidth and temporal duration of the generated microwave waveform can be changed by adjusting the amplitude and temporal duration of the control signal, respectively.

Fig. 2 shows the experimental setup of the proposed reconfigurable radar waveform generator based on an optically injected semiconductor laser. Two lasers are arranged in a

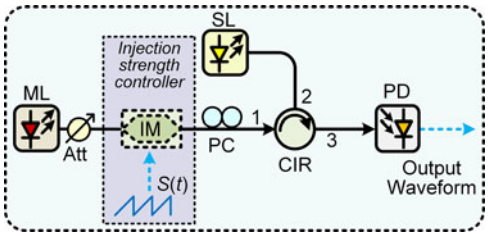

Fig. 2. Experimental setup of the proposed reconfigurable radar waveform generator based on an optically injected semiconductor laser. ML: master laser, Att: optical attenuator, IM: intensity modulator, $S(t)$: control signal, PC: polarization controller, CIR: optical circulator, PD: photodetector.

master-slave configuration for optical injection. The slave laser (Actech LD15DM) is a DFB laser biased at 31.7 mA, about 5 times of the threshold. The free-running wavelength and power of the slave laser is 1553.326 nm and 5.06 dBm, respectively. The CW light from the master laser (Agilent N7714A) passes through a variable optical attenuator, an "injection strength controller" and an optical circulator for injecting into the slave laser. The polarization of the injection light and slave laser are matched through the polarization controller. The "injection strength controller" consists of a 10 Gb/s Mach-Zehnder modulator (MZM, Lucent 2623NA) and an electrical control signal generated by a 120-MHz arbitrary waveform generator (Agilent 81150A). A 70-GHz PD (u2t XPDV3120R) is used to implement optical-to-electrical conversion. The output signal after the PD is monitored by a 32-GHz real-time oscilloscope (Keysight DSO-X 92504A) and a 50-GHz electrical spectrum analyzer (R&S FSU50). The optical spectrum is measured by an optical spectrum analyzer (Yokogawa AQ6370C) with a 0.02-nm resolution.

III. Results

Under optical injection, the dynamical behavior of a semiconductor laser can be controlled and varied by adjusting its operating parameters, including the detuning frequency and injection strength. The primary dynamical states of an optically injected semiconductor laser are stable injection locking, periodic oscillations, and chaos [12]–[13]. In the experiment, the optically injected slave laser is operated at period-one oscillation state, and the relation between period-one oscillation frequency and injection strength is first investigated. The electrical control signal is not applied and the injection strength is varied by adjusting the optical attenuator. Fig. 3(a) shows the P1 frequency f_o as a function of the injection strength ξ when detuning frequency f_i equals 5.7, 16.2, 25.7 and 35.5 GHz. As can be seen, for a fixed detuning frequency f_i, the P1 frequency f_o increases almost linearly with increasing injection strength ξ. It also can be observed that the P1 frequency increases with increasing detuning frequency for a fixed injection strength. Fig. 3(b) shows the typical optical spectrum of P1 dynamics (blue curve) when (f_i, ξ) equals to (16.2 GHz, 1.09). For comparison, the spectra of the injection light (black curve) and the free-running slave laser (red curve) are also shown. As can be seen, two highly dominant wavelength components separated by a P1 oscillation frequency of 28.8 GHz is observed after optical injection.

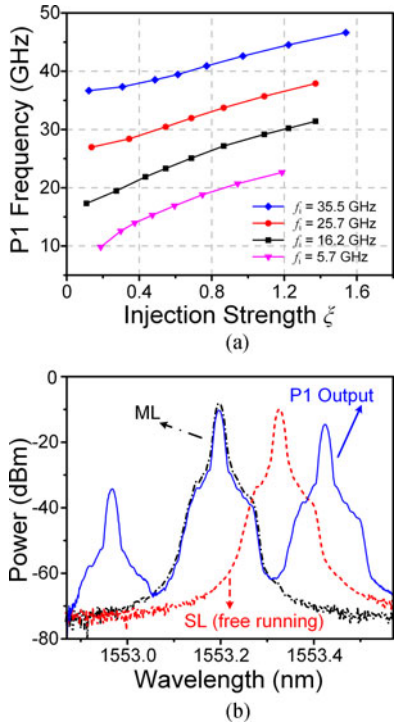

Fig. 3. (a) P1 frequency f_o as a function of the injection strength ξ for different detuning frequencies f_i. (b) Optical spectra of the injection light (black), the free-running slave laser (red), and the injected slave laser (blue) when (f_i, ξ) equals to (16.2 GHz, 1.09).

Then, the "injection strength controller" is enabled, which can generate reconfigurable radar waveforms by properly designing the control signal $S(t)$.

A. Frequency-Hopping Microwave Waveform Generation

Frequency-hopping technique is an effective method to improve the detection range and range resolution of a radar system [2], [19]. Two types of frequency-hopping microwave waveforms, i.e., stepped linear and Costas sequences, are generated using the proposed method.

To generate a frequency-hopping microwave waveform, the control signal $S(t)$ should be a multi-level signal. The detuning frequency f_i is ~5.7 GHz, and the initial injection strength is set to ~0.6. At first, a 10-MHz 4-level control signal with an amplitude of ~2.2 V is applied to the MZM to control the injection strength, which is biased at the quadrature point. At the output of PD, a frequency-hopping microwave waveform with four frequencies is obtained. As shown in Fig. 4(a-i), to obtain a 4-level stepped linear sequence, the control signal is designed to have unevenly spaced levels to compensate for the nonlinear amplitude transfer function in the MZM and elsewhere [17], [18]. Fig. 4(a-ii) and (a-iii) are the measured temporal waveform and calculated instantaneous frequency using short-time Fourier transform (STFT). As can be seen, a 4-level stepped linear sequence with a temporal period of 0.1 μs is measured. The four frequencies are 10.3, 13.8, 17.3 and 20.8 GHz. Then, by simply increasing the levels of the electrical control signal $S(t)$, the sequence length of the generated FH sequences can

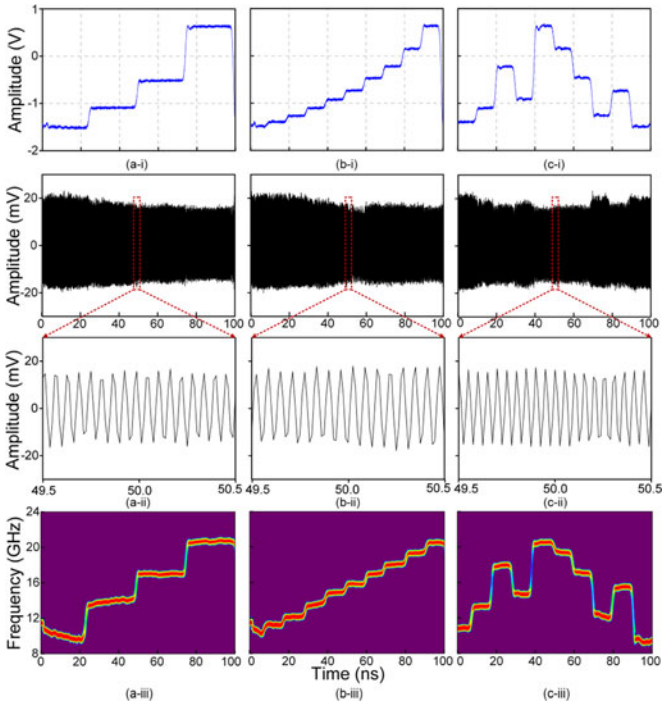

Fig. 4. (α-i) Measured control signal $S(t)$, (α-ii) measured temporal waveform, (α-iii) the recovered instantaneous frequency. α equals to a, b and c, for generating stepped linear sequence with a length of 4, 10 and Costas sequence with a length of 10.

be increased. As shown in Fig. 4(b), a 10-level stepped linear sequence is also generated, and 10 linearly increased frequency steps are observed. On the other hand, the frequency order of the frequency-hopping sequences can also be adjusted. One example is the generation of Costas sequence, which is proven to have an optimal (thumbtack-like) auto-ambiguity function and higher range-Doppler resolution [2], [19]. The control signal in Fig. 4(c-i) is applied to the MZM, and 10-level Costas sequence is generated with its waveform and instantaneous frequency separately plotted in Fig. 4(c-ii) and Fig. 4(c-iii). As can be seen, 10 frequency steps are evenly spaced between ~10 GHz and ~20.5 GHz and they transit according to the ordering of a length 10 Costas sequence, e.g., 2, 4, 8, 5, 10, 9, 7, 3, 6, 1.

B. Linearly Chirped Microwave Waveform Generation

A linearly chirped microwave waveform (LCMW) is one of the most commonly used radar waveforms and has been widely employed in the modern radar system to achieve a large detection range and a high range resolution based on pulse compression technology [2]. To generate an LCMW, the control signal $S(t)$ is set to have a near-sawtooth profile, and the injected light would have a linearly increased optical amplitude and a linearly increased injection strength ξ. The detuning frequency f_i is ~5.7 GHz. As shown in Fig. 5(a), a 1-MHz control signal with an amplitude of ~2.5 V is applied to the MZM to control the injection strength. Here, the electrical control signal S(t) is also designed to compensate the nonlinearity of amplitude transfer function in the system [17], [18]. At the output of the PD, an LCMW with a temporal period of 1 μs is generated.

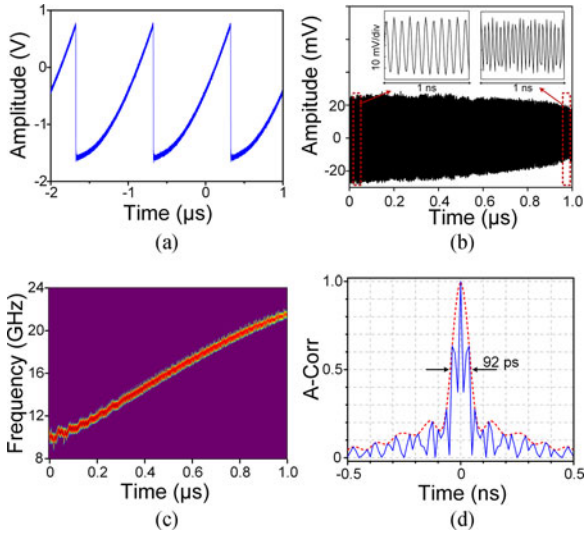

Fig. 5. (a) Measured control signal $S(t)$ with three periods, (b) measured waveform of the generated LCMW with one period (Insets: zoom-in views in temporal duration of 1 ns), (c) recovered instantaneous frequency, (d) calculated autocorrelation result.

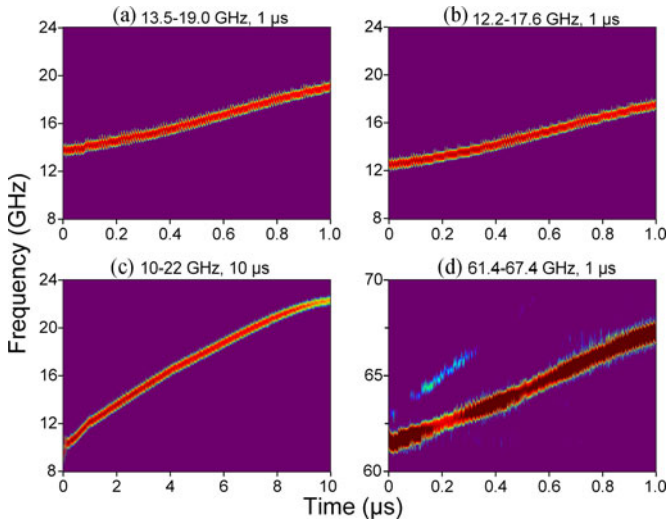

Fig. 6. STFT analysis of the generated LCMWs with (a) varied bandwidth, (b) central frequency, (c) temporal duration, and (d) frequency band.

Fig. 5(b) and (c) show the measured waveform and recovered instantaneous frequency of the generated LCMW. In Fig. 5(b), the insets show the zoom-in waveforms at the beginning and end of each period. As can be seen, the LCMW is centered at 16 GHz with a bandwidth of 12 GHz (from 10 GHz to 22 GHz). According to the result, the time-bandwidth product (TBWP) of the generated LCMW is 1.2×10^4. To demonstrate the pulse compression capability, autocorrelation of the generated LCMW is calculated, as shown in Fig. 5(d). The autocorrelation peak has a full width at half maximum (FWHM) of 92 ps, indicating a pulse compression ratio of 10870.

As explained in Section II, the central frequency, bandwidth, temporal duration, and frequency band of the generated microwave waveform are controllable. Compared to the results in Figs. 5, 6(a)–(d) show the STFT analysis of the generated signal

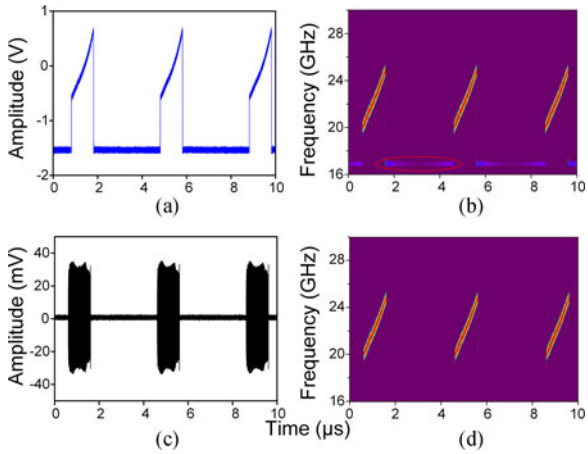

Fig. 7. (a) Measured control signal $S(t)$, (b) STFT analysis of the generated linearly chirped pulse trains before HPF, (c) measured waveform and (d) STFT analysis of the generated linearly chirped pulse trains after HPF.

with varied bandwidth, central frequency, temporal duration, and frequency band. As shown in Fig. 6(a), bandwidth of the generated LCMW is changed to 5.5 GHz (13.5–19.0 GHz) by simply adjusting the amplitude of the electrical control signal to ~1.6 V. By simply changing the initial injection strength from ~0.9 to ~0.75, the central frequency of the generated LCMW is tuned from 16.25 GHz to 14.9 GHz with a bandwidth of 5.4 GHz (12.2–17.6 GHz), as shown in Fig. 6(b). Then, by further properly configuring the control signal $S(t)$, e.g., slowing down the tuning speed of $S(t)$ to 100 kHz, an LCMW with a time duration of 10 μs with a bandwidth of 12 GHz (10-22 GHz) is generated. As can be seen in Fig. 6(c), the generated LCMW has an ultra large TBWP of about 1.2×10^5, which is significantly larger than most of the previously reported schemes. Furthermore, by increasing the master-slave detuning frequency f_i from ~5.7 GHz to ~60.4 GHz, an LCMW operating at V band is obtained. As can be seen in Fig. 6(d), the instantaneous frequency is linearly increased from 61.4 to 67.4 GHz in a 1-μs period. Because of the limited bandwidth of our oscilloscope, the generated LCMW at V band is first down-converted by a 60 GHz local oscillator (LO) signal and amplified by an intermediate frequency (IF) amplifier (DC-7 GHz), before being measured at the oscilloscope. The nonlinearity of mixing and amplification lead to some deterioration of the signal quality, such as spurs and frequency fluctuations in the instantaneous frequency.

C. Pulsed Microwave Waveform Generation

The generated frequency-hopping and linearly chirped microwave waveforms in Sections III-A and III-B are temporally continuous. In radar system, pulsed microwave waveforms are generally more preferred for realizing an integrated transceiver [2]. Next, we will show that our proposed reconfigurable microwave waveform generator can be easily adapted to generate pulsed microwave waveform by modifying the control signal or inserting an optical switch.

Fig. 7(a) shows the applied 250-kHz control signal $S(t)$ for generating linearly chirped pulse trains. The basic idea is that the low-level part of $S(t)$ is set to match with minimum transmission point (MITP) of the MZM so that the optical injection strength is negligibly weak to excite period-one oscillation at that time, while the near-sawtooth part is used to excite linearly increased P1 frequency. Fig. 7(b) shows the STFT analysis of the generated linearly chirped pulse trains with a temporal duration of 1 μs and a repetition rate of 250 kHz. In the experiment, due to the limited extinction ratio (typically 17 dB) and the bias drifting of our MZM, the low-level part of $S(t)$ still excited a periodic oscillation in the slave laser. As can be seen, a relatively weak 16.9-GHz component is observed in the time gaps between desired pulses. This problem can be solved by using a modulator with higher extinction ratio and/or a bias control circuit. A high-pass filter (HPF) can also be employed to block the low-frequency component to achieve the desired pulse trains. Fig. 7(c) and (d) shows the generated linearly chirped pulse trains and its STFT analysis after using a 19.2-GHz HPF. As expected, the generated pulses possess a temporal duration of 1 μs and a duty cycle of 25%. As shown in Fig. 7(d), a frequency coverage of 20-24.7 GHz is observed.

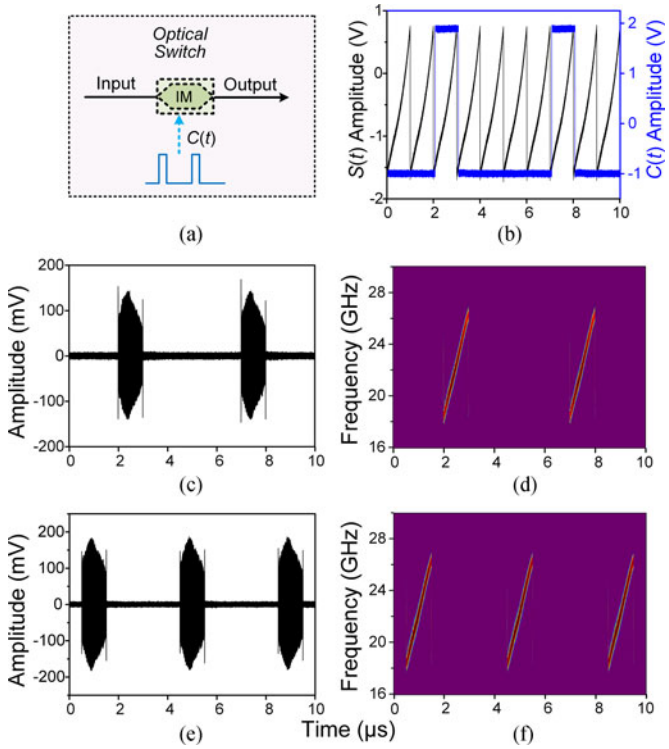

Fig. 8. (a) Schematic of the optical switch, (b) measured control signal $S(t)$ (black) and switching signal $C(t)$ (blue), (c) measured waveform and (d) STFT analysis of the generated linearly chirped pulse trains with a repetition rate of 200 kHz, (e) measured waveform and (f) STFT analysis of the generated pulse trains with a repetition rate of 250 kHz.

By inserting an optical switch before the PD in Fig. 2, pulsed microwave waveforms can be generated. For example, using an electro-optical intensity modulator driven by a periodic switching signal to function as an optical switch, pulsed microwave waveforms are obtained, as shown in Fig. 8(a). Fig. 8(b) is the measured 1-MHz control signal $S(t)$ (black) in the "injection strength controller" and the 200-kHz switching signal $C(t)$

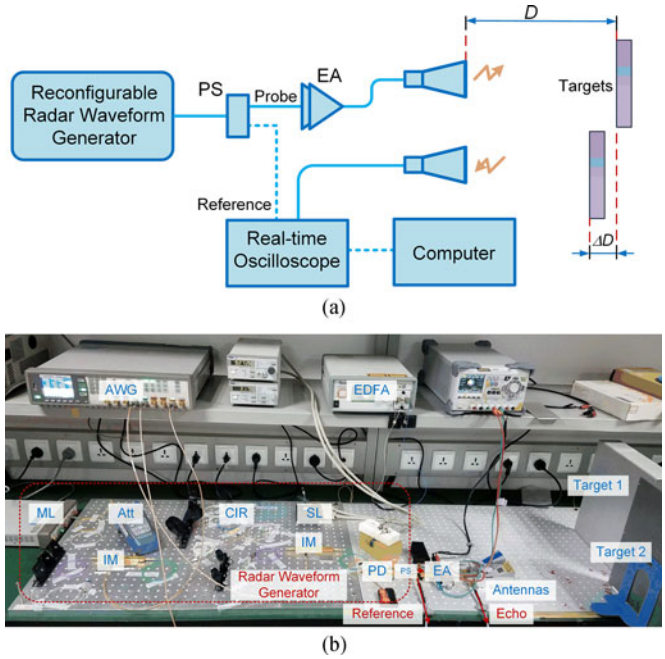

Fig. 9. (a) Schematic setup and (b) photograph of a radar system based on an optically injected semiconductor laser. PS: power splitter, EA: electrical amplifiers, AWG: arbitrary waveform generator.

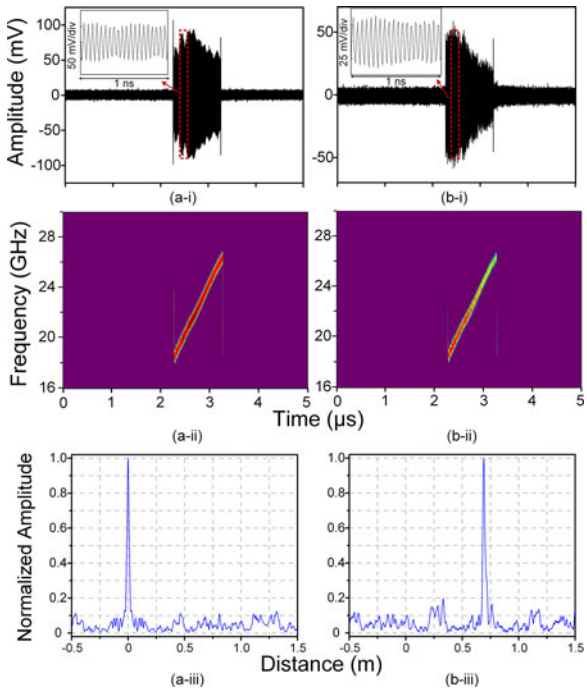

Fig. 10. (a-i) Temporal waveform, (a-ii) STFT analysis and (a-iii) autocorrelation of the transmitted signal. (b-i) Temporal waveform, (b-ii) STFT analysis of the received signal and (b-iii) correlation between transmitted/received waveform. (Insets: zoom-in views in temporal duration of 1ns).

(blue) in the optical switch. Fig. 8(c) and (d) shows the generated linearly chirped pulse trains and its STFT analysis. As can be seen, the generated pulses possess a temporal duration of 1 μs and a duty cycle of 20%. As shown in Fig. 8(d), the generated pulses cover a frequency range of 18.3–26.4 GHz, nearly full K-band (18–26.5 GHz). In addition, by simply adjusting the repetition rate of switching signal $C(t)$ to 250 kHz, the resultant repetition rate of the generated pulses is changed to 250 kHz, while the temporal duration of 1 μs and frequency coverage are maintained, as shown in Fig. 8(e) and (f).

D. Radar Detection Ability

To further investigate the performance of the proposed radar waveform generator based on an optically injected semiconductor laser, its application in a radar system is experimentally studied in our laboratory. The schematic setup and photograph of the radar system based on an optically injected semiconductor laser are shown in Fig 9. In the experiment, linearly chirped pulses are generated from the reconfigurable radar waveform generator. Here, the optical switch method in Section III-C is adopted for pulse generation. The linearly chirped pulses then split into two channels, the probe and the reference. The probe signal is amplified by cascaded electrical amplifiers with a total gain of ~46 dB and then transmitted by a horn antenna. After air transmission and reflected by the target(s), the probe signal is received by another antenna. The received probe signal together with the reference signal are recorded simultaneously by a real-time oscilloscope, where target detection and localization are accomplished through correlation. The antennas used in the experiment have a bandwidth of 18–26.5 GHz (i.e., K band), and the transmitted signal is a 1-μs linearly chirped pulses trains with a repetition of 200 kHz and a frequency range of 18.3–26.4 GHz.

Firstly, a single-target detection experiment is conducted. Fig. 10(a-i) and (b-i) show the transmitted and received waveforms in 5 μs when the actual distance between the antenna pair and the target is 42.40 cm, where the insets show the zoom-in waveforms of 1ns around 2.5 μs. Fig. 10(a-ii) and (b-ii) are the recovered instantaneous frequency of the transmitted and received waveforms, showing that the linearly chirped feature has been well-retained. No obvious time-delay is observed by directly comparing the transmitted and received waveforms. To precisely acquire the time delay and distance, autocorrelation of the transmitted linearly chirped pulse and cross-correlation between the transmitted/received waveforms are calculated, as shown in Fig. 10(a-iii) and (b-iii). By calculating the difference between the two correlation peaks and subtracting a fixed length of cables and other components, the desired distance between the antenna pair and the target can be achieved. For the circumstance in Fig. 10, the measured distance d is 42.47 cm while the actual distance D is 42.40 cm, leading to a measurement error of 0.07 cm. In the experiment, multiple distance measurements are performed by changing the target position, the results (D, d) are: (42.40 cm, 42.47 cm), (30.05 cm, 30.10 cm), (16.82 cm, 16.80 cm), (90.03 cm, 90.03 cm) and (46.25 cm, 46.78 cm). The measurement error is found to be 0.07 cm, 0.05 cm, 0.02 cm, 0 cm and 0.53 cm, respectively.

Then, the range resolution of the radar system is investigated by performing a dual-target detection experiment. As illustrated in the setup in Fig. 9, two metal plates are placed side by side but separated by a distance of ΔD along the ranging direction. The same K-band linearly chirped microwave waveform for single-target detection is used again. Fig. 11(a) and (c) show the received signals when ΔD is changed, and the insets

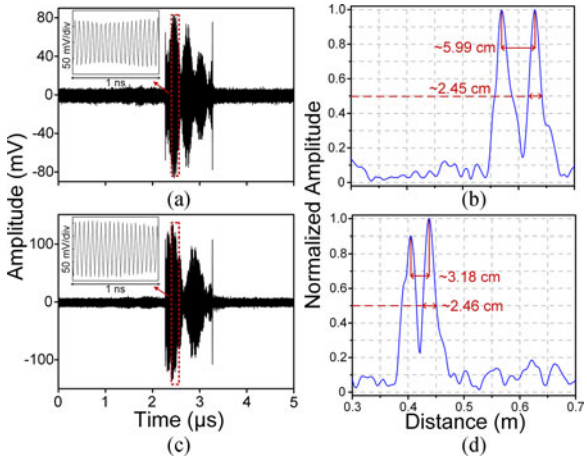

Fig. 11. Temporal waveforms the received signals when the distance between the two targets is (a) 5.99 cm and (b) 3.18 cm, the cross-correlation results when the distance between the two targets is (c) 5.99 cm and (d) 3.18 cm. (Insets: zoom-in views in temporal duration of 1ns).

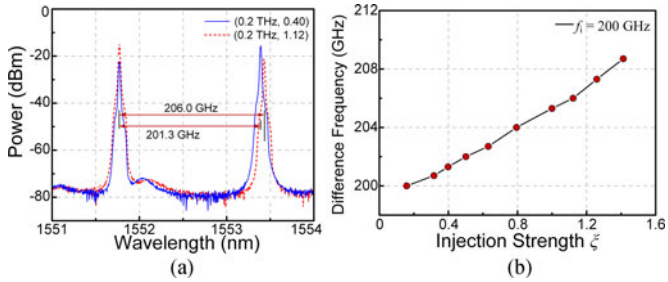

Fig. 12. Measured results when $f_{\mathrm{i}} = 200\,\mathrm{GHz}$. (a) Output spectra when ξ equals to 0.40 (blue) and 1.12 (red), (b) Measured difference frequency f_{o} as a function of the injection strength ξ.

are the zoom-in waveforms of 1ns around 2.5 μs. As can be seen, the reflected signals from two targets are hard to distinguish without signal processing. After performing the matched filtering processing, i.e., calculating the cross-correlation between the transmitted/received waveforms, two reflection peaks are clearly distinguished in the ranging results, as depicted in Fig. 11(b) and (d). The measured distance between these two peaks indicates the distance between the targets. Fig. 11(b) and (d) correspond to the circumstances when the distance between the two targets (ΔD) is 5.99 cm and 3.18 cm, respectively. On the other hand, the FWHM of the cross-correlation peak (i.e., $\sim$2.45 cm and $\sim$2.46 cm) is approximately equal to each other, and indicates that the range resolution of our radar system is $\sim$2.46 cm. It should be noted that the performance of our radar system can be enhanced by improving the phase noise performance and amplitude uniformity of the generated radar waveforms. The generated microwave using optically injected semiconductor laser has a relatively large 3-dB linewidth on the order of megahertz, which is mainly caused by the spontaneous emission noise of the injected laser. In this work, the measured linewidth for generated P1 signal is measured to be $\sim$200 kHz. This problem can be solved by using an optoelectronic feedback structure. For example, in [20], the microwave phase noise of generated frequency-modulated continuous-wave (FMCW) signals is successfully reduced by adding a delay-matched optoelectronic feedback loop. Besides, the uneven amplitude of transmitted waveforms will lead to a slightly degraded range resolution. This problem can be solved by using either electrical or optical power limiting techniques. For instance, in [24], an optical limiting amplifier is used to compensate the amplitude variation.

IV. Discussion

A. Extending the Frequency Range Towards THz Band

In the aforementioned experiments, by introducing intensity modulation to the injection strength of an optically injected semiconductor laser, reconfigurable radar waveforms are generated covering a wide frequency range from several GHz to $\sim$67 GHz, corresponding to frequency bands from X-band to V-band. To the best of our knowledge, this is the largest frequency coverage of waveform generation using semiconductor lasers. Recently, terahertz (THz) frequency band (0.1–10 THz) has attracted increasing attentions for novel radar applications in recent years. For instance, linearly chirped waveforms at THz band are required for real-time THz imaging systems using synthetic aperture radar (SAR) techniques [25]. Compared to radar imaging system at microwave/millimeter wave bands, THz radar imaging system has a higher resolution and a shorter imaging time.

TABLE I
The Tuning Range of Difference Frequency for Different Detuning Frequency

Detuning frequency f_i (GHZ)	Difference frequency f_o (GHz)	Variation of f_o (GHz)
101	101–110	9
200	200–208.7	8.7
400	400–406.6	6.6
1000	1000–1004.5	4.5

In this study, the circumstances when the master-slave detuning frequency f_{i} is larger than 100 GHz are investigated for THz signal generation using optically injected semiconductor lasers. The detuning frequency f_{i} is first set to 200 GHz and the optical spectra are shown in Fig. 12(a) when ξ equals to 0.40 (blue curve) and 1.12 (red curve). As can be seen, two highly dominant wavelength components separated by 201.3 GHz and 206.0 GHz are observed after optical injection. The difference frequency f_{o} between the two components as a function of the injection strength ξ is also measured, as shown in Fig. 12(b). In this process, when the injection strength increases from 0.16 to 1.41, the corresponding difference frequency f_{o} can be tuned from 200 GHz to 208.7 GHz. Then, the tuning range of difference frequency f_{o} for different detuning frequency f_{i} are investigated and the results are displayed in Table I. As can be seen, when f_{i} equals to 101, 200, 400 and 1000 GHz, the achievable tuning bandwidth of f_{o} is 9, 8.7, 6.6 and 4.5 GHz, respectively. When $f_{\mathrm{i}} = 2$ THz, the achievable tuning bandwidth of f_{o} is further decreased to less than 2 GHz. The decrease

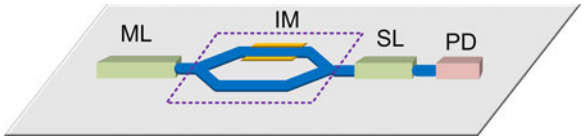

Fig. 13. Schematic diagram of an on-chip radar waveform generator.

of bandwidth can be explained by that the antiguidance effect or the gain reduction in the injected laser becomes weaken with the increase of detuning frequency. This indicates that if a PD with higher bandwidth is employed, THz signal with tunable frequency can be generated. Therefore, by setting the injected light to have a linearly increased optical amplitude using the method in Section II, the generated THz signal will also have a linearly increased instantaneous frequency, i.e., linearly chirped waveform at THz band can be generated, which may find wide applications in THz radar system.

B. Integration Possibility

Compared with photonic signal generation schemes using devices such as a spatial light modulator, a fabricated FBG, a femtosecond pulsed laser, a high-speed EOM or a high-speed electrical AWG, the proposed approach only needs a commercial semiconductor laser and a low-speed intensity modulator. Since the intensity modulator in the system can be implemented using an integrated modulator, e.g., an electro-absorption modulator (EAM), the proposed LCMW generator can have a very compact structure. Furthermore, it can be improved to realize an on-chip reconfigurable radar waveform generator based on optically injected semiconductor lasers. Fig. 13 gives a schematic diagram of the on-chip radar waveform generator. It should be noted that, the bandwidth requirement of the intensity modulator is no more than 100 MHz in our system, making the integrated intensity modulator easier to implement. The only high-speed component is the PD, which is reported to have a bandwidth as large as several hundreds of GHz [26], [27]. Therefore, our approach can provide a possible scheme to the on-chip reconfigurable radar waveform generator.

V. Conclusion

An approach to generating reconfigurable radar waveforms is proposed and demonstrated based on an optically injected semiconductor laser. In the proposed system, the period-one oscillation frequency (e.g., the output microwave frequency) of the injected laser can be dynamically controlled by simply manipulating the injection strength using a low-speed control signal. By properly designing the control signal, reconfigurable radar waveforms with desired properties and parameters can be generated. Experiments are carried out to generate frequency-hopping microwave waveforms, linearly chirped microwave waveforms, and pulsed microwave waveforms. The parameters of these radar waveforms are also proved to be adjustable, including the central frequency, bandwidth, temporal duration, frequency band, and duty cycle. The generated radar waveforms can achieve a frequency coverage from ~10 to ~67 GHz (or possibly several THz), a bandwidth larger than 10 GHz, a time-bandwidth product as large as 1.2×10^5. In addition, the proposed radar waveform generator based on the optically injected semiconductor laser is tested in a radar system, a ranging accuracy of less than 1 cm and a resolution of ~2.46 cm is obtained. The proposed waveform generator features low cost, simple structure, and high performance, which can find applications in modern radar systems.

References

[1] M. K. Simon, J. K. Omura, R. A. Scholtz, and B. K. Levitt, *Spread Spectrum Communications Handbook*. New York, NY, USA: McGraw-Hill, 1994.
[2] M. I. Skolnik, *Radar Handbook*, 3rd ed. New York, NY, USA: McGraw-Hill, 2008.
[3] S. L. Pan, D. Zhu, and F. Z. Zhang, "Microwave photonics for modern radar systems," *Trans. Nanjing Univ. Aeronaut. Astronaut.*, vol. 31, no. 3, pp. 219–240, Jun. 2014.
[4] G. C. Tavik *et al.*, "The advanced multifunction RF concept," *IEEE Trans. Microw. Theory Tech.*, vol. 53, no. 3, pp. 1009–1019, Mar. 2005.
[5] E. D. Adler, E. A. Viveiros, T. Ton, J. L. Kurtz, and M. C. Bartlett, "Direct digital synthesis applications for radar development," in *Proc. 1995 IEEE Int. Radar Conf.*, 1995, pp. 224–226.
[6] A. Krishnan *et al.*, "Reconfigurable direct space-to-time pulse-shaper based on arrayed waveguide grating multiplexers and digital micromirrors," *IEEE Photon. Technol. Lett.*, vol. 17, no. 9, pp. 1959–1961, Aug. 2005.
[7] A. Vega, D. E. Leaird, and A. M. Weiner, "High-speed direct space-to-time pulse shaping with 1 ns reconfiguration," *Opt. Lett.*, vol. 35, no. 10, pp. 1554–1556, May 2010.
[8] C. Wang and J. P. Yao, "Photonic generation of chirped millimeter-wave pulses based on nonlinear frequency-to-time mapping in a nonlinearly chirped fiber Bragg grating," *IEEE Trans. Microw. Theory Tech.*, vol. 56, no. 2, pp. 542–553, Feb. 2008.
[9] F. Z. Zhang, X. Z. Ge, S. L. Pan, and J. P. Yao, "Photonic generation of pulsed microwave signals with tunable frequency and phase based on spectral-shaping and frequency-to-time mapping," *Opt. Lett.*, vol. 38, no. 20, pp. 4526–4529, Oct. 2013.
[10] W. Li, F. Kong, and J. P. Yao, "Arbitrary microwave waveform generation based on a tunable optoelectronic oscillator," *J. Lightw. Technol.*, vol. 31, no. 23, pp. 3780–3786, Dec. 2013.
[11] Y. M. Zhang, X. W. Ye, Q. S. Guo, F. Z. Zhang, and S. L. Pan, "Photonic generation of linear frequency-modulated waveforms with improved time-bandwidth product based on polarization modulation," *J. Lightw. Technol.*, vol. 35, no. 10, pp. 1821–1829, May 2017. [Online]. Available: http://ieeexplore.ieee.org/document/7814254/
[12] S. K. Hwang, J. M. Liu, and J. K. White, "Characteristics of period-one oscillations in semiconductor lasers subject to optical injection," *IEEE J. Sel. Topics Quantum Electron.*, vol. 10, no. 5, pp. 974–981, Sep. 2004.
[13] S. C. Chan, R. Diaz, and J. M. Liu, "Novel photonic applications of nonlinear semiconductor laser dynamics," *Opt. Quantum Electron.*, vol. 40, no. 5, pp. 83–95, Mar. 2008.
[14] S. C. Chan, S. K. Hwang, and J. M. Liu, "Radio-over-fiber AM-to-FM upconversion using an optically injected semiconductor laser," *Opt. Lett.*, vol. 31, no. 15, pp. 2254–2256, Aug. 2006.
[15] S. C. Chan, "Analysis of an optically injected semiconductor laser for microwave generation," *IEEE J. Quantum Electron.*, vol. 46, no. 3, pp. 421–428, Mar. 2010.
[16] P. Zhou, F. Z. Zhang, B. D. Gao, and S. L. Pan, "Optical pulse generation by an optoelectronic oscillator with optically injected semiconductor laser," *IEEE Photon. Technol. Lett.*, vol. 28, no. 17, pp. 1827–1830, Sep. 2016.
[17] M. Pochet, N. A. Naderi, Y. Li, V. Kovanis, and L. F. Lester, "Tunable photonic oscillators using optically injected quantum-dash diode lasers," *IEEE Photon. Technol. Lett.*, vol. 22, no. 11, pp. 763–765, Jun. 2010.
[18] P. Zhou, F. Z. Zhang, Q. S. Guo, and S. L. Pan, "Linearly chirped microwave waveform generation with large time-bandwidth product by optically injected semiconductor laser," *Opt. Express*, vol. 24, no. 16, pp. 18460–18467, Aug. 2016.
[19] P. Zhou, F. Z. Zhang, X. W. Ye, Q. S. Guo, and S. L. Pan, "Flexible frequency-hopping microwave generation by dynamic control of optically injected semiconductor laser," *IEEE Photon. J.*, vol. 8, no. 6, Dec. 2016, Art. no. 5501909.

[20] J. P. Zhuang, X. Z. Li, S. S. Li, and S. C. Chan, "Frequency-modulated microwave generation with feedback stabilization using an optically injected semiconductor laser," *Opt. Lett.*, vol. 41, no. 24, pp. 5784–5787, Dec. 2016.
[21] Y. H. Hung and S. K. Hwang, "Photonic microwave amplification for radio-over-fiber links using period-one nonlinear dynamics of semiconductor lasers," *Opt. Lett.*, vol. 38, no. 17, pp. 3355–3358, Sep. 2013.
[22] Y. H. Hung, C. H. Chu, and S. K. Hwang, "Optical double-sideband modulation to single-sideband modulation conversion using period-one nonlinear dynamics of semiconductor lasers for radio-over-fiber links," *Opt. Lett.*, vol. 38, no. 9, pp. 1482–1484, May 2013.
[23] S. K. Hwang, H. F. Chen, and C. Y. Lin, "All-optical frequency conversion using nonlinear dynamics of semiconductor lasers," *Opt. Lett.*, vol. 34, no. 6, pp. 812–814, Mar. 2009.
[24] J. W. Shi *et al.*, "Photonic generation and wireless transmission of linearly/nonlinearly continuously tunable chirped millimeter-wave waveforms with high time-bandwidth product at W-band," *IEEE Photon. J.*, vol. 4, no. 1, pp. 215–223, Feb. 2012.
[25] J. Ding, M. Kahl, O. Loffeld, and P. H. Bolivar, "THz 3-D image formation using SAR techniques: Simulation, processing and experimental results," *IEEE Trans. THz Sci. Technol.*, vol. 3, no. 5, pp. 606–616, Sep. 2013.
[26] X. B. Yu *et al.*, "400-GHz wireless transmission of 60-Gb/s Nyquist-QPSK signals using UTC-PD and heterodyne mixer," *IEEE Trans. THz Sci. Technol.*, vol. 6, no. 6, pp. 765–760, Nov. 2016.
[27] F. N. Xia, T. Mueller, Y. M. Lin, A. Valdes-Garcia, and P. Avouris, "Ultrafast graphene photodetector," *Nature Nanotech.*, vol. 4, pp. 839–843, Oct. 2009.

Pei Zhou (S'15) received the B.S. degree in electronic science and technology from Nanjing University of Aeronautics and Astronautics (NUAA), Nanjing, China, in 2013. He is currently working toward the Ph.D. degree in the Key Laboratory of Radar Imaging and Microwave Photonics, NUAA, Ministry of Education.

His current research interests include application of nonlinear laser dynamics, and microwave photonic signal generation.

Fangzheng Zhang (S'10–M'13) received the B.S. degree from Huazhong University of Science and Technology, Wuhan, China, and the Ph.D. degree from Beijing University of Posts and Telecommunications, Beijing, China, in 2008 and 2013, respectively.

He is currently working as an Associate Professor in the College of Electronic and Information Engineering, Nanjing University of Aeronautics and Astronautics, Nanjing, China. His main research interests include microwave photonics, coherent optical communications, and all-optical signal processing.

Qingshui Guo received the B.S. degree in electronic science and technology from Nanjing University of Aeronautics and Astronautics (NUAA), Nanjing, China, in 2015. He is currently working toward the Master's degree in the Key Laboratory of Radar Imaging and Microwave Photonics, NUAA, Ministry of Education.

His main research interest focuses on microwave photonic signal generation.

Simin Li received the B.S. and Ph.D. degrees from Nanjing University, Nanjing, China, in 2009 and 2014, respectively.

She is currently working in the Key Laboratory of Radar Imaging and Microwave Photonics, Nanjing University of Aeronautics and Astronautics, Ministry of Education, Nanjing, China. Her main research interest focuses on integrated microwave photonics.

Shilong Pan (S'06–M'09–SM'13) received the B.S. and Ph.D. degrees in electronics engineering from Tsinghua University, Beijing, China, in 2004 and 2008, respectively.

From 2008 to 2010, he was a "Vision 2010" Postdoctoral Research Fellow in the Microwave Photonics Research Laboratory, University of Ottawa, Ottawa, ON, Canada. In 2010, he joined the College of Electronic and Information Engineering, Nanjing University of Aeronautics and Astronautics, Nanjing, China, where he is currently a Full Professor and the Deputy Director of the Key Laboratory of Radar Imaging and Microwave Photonics, Nanjing University of Aeronautics and Astronautics, Ministry of Education. He has authored or co-authored more than 290 research papers, including more than 150 papers in peer-reviewed journals and 140 papers in conference proceedings. His research has focused on microwave photonics, which includes optical generation and processing of microwave signals, ultra-wideband over fiber, photonic microwave measurement, and integrated microwave photonics.

Dr. Pan is a Senior Member of the IEEE Microwave Theory and Techniques Society, the IEEE Photonics Society, the IEEE Instrumentation and Measurement Society, and a member of the Optical Society of America. He was selected to receive an OSA outstanding reviewer award in 2015. He is currently a Topical Editor for *Chinese Optics Letters*. He was a Chair of numerous international conferences and workshops, including the TPC Chair of the IEEE ICOCN 2015, TPC Chair of the high speed and broadband wireless technologies subcommittee of the IEEE Radio Wireless Symposium in 2013, 2014, and 2016, TPC Chair of the Optical fiber sensors and microwave photonics subcommittee chair of the Optoelectronics and Communication Conference in 2015, a Chair of the microwave photonics for broadband measurement workshop of International Microwave Symposium in 2015, a TPC Chair of the microwave photonics subcommittee of CLEO-PR, OECC, and PGC 2017 (joint conference), and a TPC Co-Chair of the IEEE MWP 2017.